Anisotropic dewetting polydimethylsiloxane surface fabricated using ultrashort laser pulses

Huaihai Pan (泮怀海)[1,2], Fangfang Luo (骆芳芳)[3], Geng Lin (林 耿)[1,2], and Quanzhong Zhao (赵全忠)[1,*]

[1]*State Key Laboratory of High Field Laser Physics, Shanghai Institute of Optics and Fine Mechanics, Chinese Academy of Sciences, Shanghai 201800, China*

[2]*Graduate University of the Chinese Academy of Sciences, Beijing 100049, China*

[3]*Department of Electrical and Computer Engineering, National University of Singapore, Singapore 117576, Singapore*

**Corresponding author: zqz@siom.ac.cn*

Received October 20, 2014; accepted January 16, 2015; posted online March 13, 2015

Anisotropic dewetting polydimethylsiloxane (PDMS) surfaces, which consist of groove-like micro/nanostructures (so-called hierarchical structures), are fabricated using an ultrashort pulsed laser. The contact angles (CAs) are measured parallel to the microgrooves, which are always larger than those measured perpendicular to the microgrooves, exhibiting a superhydrophobic anisotropy of approximately 4° on these fabricated PDMS surfaces at optimized parameters. These pulsed-laser irradiated surfaces exhibit enhanced hydrophobicity with CAs that increase from 116° to 156° while preserving the anisotropic dewetting. Additionally, the wettability of the surfaces with different morphologies is investigated. The temporal evolution of the wettability of the pulsed-laser irradiated PDMS surface is also observed within the first few hours after pulsed laser irradiation.

OCIS codes: 140.3390, 140.3538, 160.1435, 160.4236.
doi: 10.3788/COL201513.031404.

Inspired by natural special surfaces, such as self-cleaning lotus leaves[1], iridescent butterfly wings[2], antireflection moth eyes[3], and anisotropic rice leaves[4], researchers have attempted to fabricate biomimetic surfaces with special functions. Among these surfaces with special functions, surfaces of superhydrophobicity with a contact angle (CA) exceeding 150° have elicited extensive interest because of their potential applications in self-cleaning surfaces[1], drug delivery[5], and cell cultures[6], as well as in micro-fluidic devices for bio-assays[7]. According to the models of Refs. [8,9], the superhydrophobicity can be achieved by a cooperative effect of lowering the surface energy and fabricating rough surfaces consisting micro/nanostructures. Until now, various techniques have been employed to fabricate superhydrophbic surfaces, e.g. plasma coating[10], electrospinning[11], and photolithographic techniques[12]. However, these techniques have some shortcomings such as multi-steps or time-consuming. In order to simplify the process of fabricating micro/nanostructures with superhydrophobic properties, a simple, novel method is required. Ultrashort pulsed laser irradiation[13–17] has been developed for inducing micro/nanostructures on surfaces because of its ignorable thermal effect in the process of interaction with materials. In this technique, a pulsed laser beam can be focused to a small diameter within several micrometers by using a microscope objective, which makes the pulsed laser a suitable tool to fabricate micro/nanostructures on surface of low surface energy and consequently to achieve superhydrophobic surface.

In this work, a pulsed laser was utilized to precisely control the dimensions at the micro-scale while producing anisotropic superhydrophobic micro/nanostructures by using only one simple step (i.e., pulsed laser direct writing) on polydimethylsiloxane (PDMS) surfaces. This gives us a better understanding on the superhydrophobic properties of surfaces with different morphologies. PDMS was employed because of its unique properties, such as flexibility, optical transparency above 230 nm, and biocompatibility, as well as chemical and thermal stability. The morphology of the fabricated surfaces was characterized by a scanning electron microscope (SEM). Additionally, the dimensions of the fabricated surfaces at micro-scale were also measured using an optical microscope, which included the width, depth, and period of the microgrooves. By tuning the laser power and pitch between two adjacent microgrooves on the pulsed-laser irradiated PDMS surfaces, surfaces with varying wettability were obtained. The temporal evolution of wettability on our fabricated PDMS surfaces by pulsed laser irradiation was also investigated. These fabricated anisotropic superhydrophobic PDMS surfaces have a great potential in micro-fluidic channel applications[18].

The PDMS sheets used in this work were purchased from Goodfellow Cambridge Limited and were cut into small pieces with dimensions of 20 mm × 20 mm × 2 mm. Before irradiation using a pulsed laser, these PDMS pieces were rinsed ultrasonically with ethanol for 5 min to remove surface contamination, and then were dried in air.

A 1 kHz regenerative amplified Ti:sapphire laser system with a central wavelength of 800 nm delivering 120 fs laser pulses was used for the surface irradiation. The laser beam output was horizontally polarized to the optical table

(in the x-direction) and focused onto a cleaned PDMS surface mounted on a 3D linear translational stage via a microscope objective (5×, NA = 0.15), where the focused laser spot diameter on the PDMS surface was approximately 13 μm. By moving the 3D linear translational stage at a fixed scanning speed of 1 mm/s in the horizontal direction across the laser beam, microgrooves with 8 mm length and different pitches were produced on the PDMS surfaces. The laser power employed was mainly in the range of 10–160 mW. This process was repeated to produce an extended array of microgrooves with an area of 8 mm × 8 mm on the PDMS surface. In summary, a series of fabricated PDMS surfaces with different morphologies was produced via the pulsed laser irradiation by tuning the laser power and pitch between two adjacent microgrooves.

After fabrication by the pulsed laser, we used a JSM 6700F SEM (JEOL, Japan) at 10.0 kV to examine the surface structures of the samples. The sample surface was coated with a thin gold film to improve electrical conductivity before the microscopic measurement. The static CA was measured with a CA measurement system (SL200B) using the sessile drop method. A micro-syringe was used to drop gently a 2 μL distilled water droplet on the surface. The images of the water droplet were captured using a CCD camera to measure the CA formed at the water–solid interface. Two types of measurements were conducted to acquire the CA data. For the first type, the average value of the CA was obtained by taking five measurements at different positions on the same sample only after about 6 h of laser irradiation to ensure the stability of the sample. For each sample position, the CA was measured in two different directions, namely in the x- and y-directions, in which the x-direction was parallel to the microgroove and the y-direction was perpendicular to the microgroove. For the second type of measurement, the temporal evolution of the CA on the irradiated samples was measured immediately after the pulsed laser irradiation. The measurement was taken for a total time of 340 min with a 10 min interval. Every measurement was obtained in the x- and y-directions. To investigate the effect of chemical changes on the wettability of PDMS surfaces, micro-Raman spectra were obtained using a Raman spectrometer (Renishaw inVia) with a 488 nm laser excitation.

Figure 1 shows SEM images of the fabricated PDMS surface in different zoom sizes, where the laser power, scanning speed, and pitch between two adjacent microgrooves were set to 30 mW, 1 mm/s, and 15 μm, respectively. In Fig. 1(a), the top part of the SEM image indicated by the dark area is the nonirradiated PDMS surface, and the bottom part is the irradiated PDMS surface by the pulsed laser. On the pulsed-laser irradiated PDMS surface, microgroove-like microstructures are formed on the surface. The magnified SEM images in Figs. 1(b) and 1(c) show an array of parallel microgrooves. The period of the microgrooves is 15 μm, which is given by the distance shift of the 3D linear translational stage. Laser-induced periodic surface structures (LIPSSs) that formed on the inner-shell wall of the microgrooves, as shown in Figs. 1(c) and 1(d), could be attributed to the absorbed laser electromagnetic field into the inner-shell wall of the microgrooves. These LIPSSs that formed on the inner-shell wall have been reported before[19], in which the laser polarization and energy just above the energy threshold were the main control parameter for formation of the LIPSS. As illustrated in Figs. 1(c) and 1(d), the LIPSS orientation could be considered to be in the direction of the microgrooves (i.e., x-direction), which is parallel to the laser polarization direction in our work. It is noted that for polymers, unlike metals, the direction of laser polarization and LIPSS orientation has a parallel correlation[20]. Hence in our case, it is obvious that these microgrooves consisting of a LIPSS that has a period of approximately 1 μm play a crucial role in enhancing the surface roughness of the fabricated PDMS.

Figure 2 shows a comparison of the CA of a water droplet between the irradiated and nonirradiated PDMS surfaces by the pulsed laser using the CCD. It is shown that the CAs of water droplets on PDMS surfaces increase from 116° [Fig. 1(a)] to 156° [Fig. 1(b)] after the pulsed laser irradiation. The wettability of materials is generally defined as hydrophilic for water CA ≤ 90°, hydrophobic for 90° < water CA < 150°, and superhydrophobic for water CA ≥ 150°. Therefore, from Fig. 2(b), the superhydrophobicity of our pulsed-laser irradiated PDMS surfaces is successfully realized under the optimal laser power

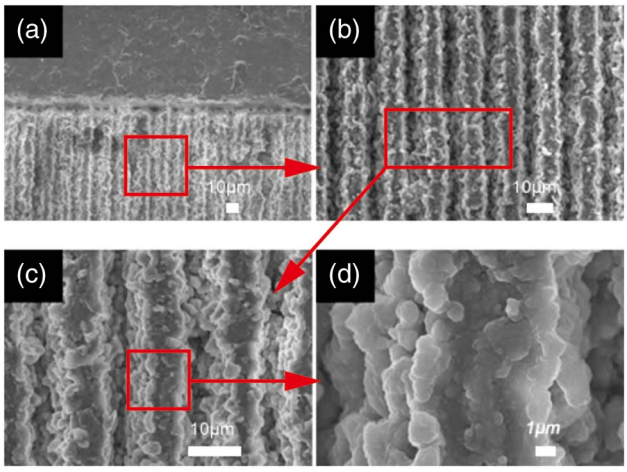

Fig. 1. SEM images of the pulsed-laser irradiated PDMS surface under different magnifications.

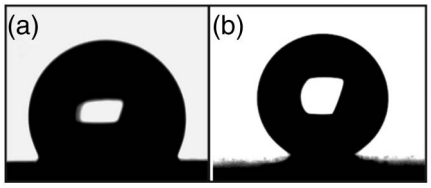

Fig. 2. (a) Side view of water droplet on the nonirradiated PDMS surface; (b) side view of water droplet on the irradiated PDMS surface at optimized conditions.

(i.e., 30 mW) and pitch size (i.e., 15 μm) between two adjacent microgrooves with a scanning speed of 1 mm/s.

To investigate the effect of rough PDMS surfaces with micro/nanostructures on the wettability, the scanning line pitch between two adjacent microgrooves was varied to change the period of the microgrooves, thus obtaining PDMS surfaces with different morphologies. In Fig. 3(a), the blue triangle shows the plot of the measured CA values versus the pitch between two adjacent microgrooves on pulsed-laser irradiated PDMS surfaces, in which the pitch varies from 20 to 400 μm with the laser power and scanning speed fixed at 10 mW and 1 mm/s, respectively. Figure 3(a) shows that the CAs decrease from 153° to 118° with the increasing of pitch. Therefore, the wettability of PDMS surfaces can be controlled by adjusting the period of the microgrooves fabricated by pulsed-laser irradiation.

As shown in Fig. 3(a), the morphology of the surface is determined by the period of the microgrooves. In order to explain the effect of morphology on the wettability of pulsed-laser irradiated PDMS, two models have been proposed[8,9]. One is the Wenzel model[8] and another is the Cassie model[9], whose diagrammatic representations are shown in Figs. 3(b) and 3(c), respectively. In the Wenzel model[8] as shown in Fig. 3(b), the CA on the rough surface can be described as follows

$$\cos\theta_e^W = r\cos\theta_e, \tag{1}$$

where r is the roughness factor (defined as the ratio of actual area wetted by liquid to the projected area of surface), θ_e^W denotes the CA on the rough surface of the Wenzel (W) state, and θ_e is the CA on a flat surface given by Young's equation

$$\cos\theta_e = \frac{\gamma_{sv} - \gamma_{sl}}{\gamma_{lv}}, \tag{2}$$

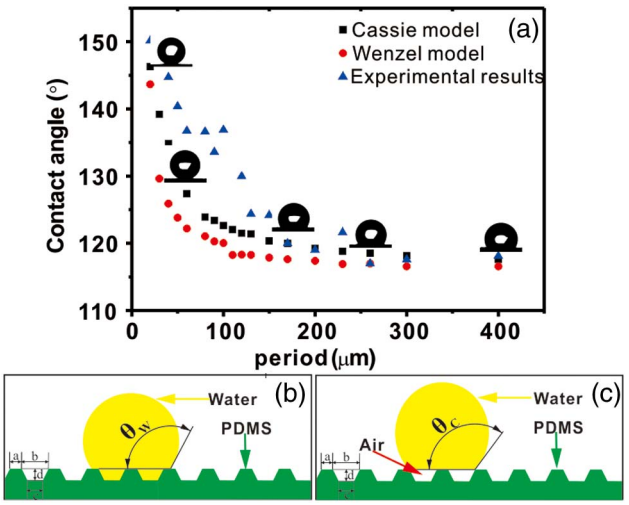

Fig. 3. (a) CA of PDMS surface as a function of period; (b) water droplet on a rough surface (Wenzel model); (c) water droplet on a rough surface (Cassie model).

where γ_{sv}, γ_{sl}, and γ_{lv} denote the surface tensions of solid–vapor contact, solid–liquid contact, and liquid–vapor contact, respectively.

The second model is the Cassie model[9] as shown in Fig. 3(c), in which the rough surface can be considered to be a composite surface consisting of solid and air fractions when a water droplet is dropped on such a rough surface, and the CA can be expressed as follows

$$\cos\theta_e^C = f\cos\theta_e + f - 1, \tag{3}$$

where f represents the solid area fraction wetted by liquid ($f < 1$), and θ_e^C denotes the CA of water droplet on the rough surface when it is in the Cassie state.

Based on Eqs. (1) and (3), it is shown that wettability is heavily dependent on the roughness factor described as follows

$$r = \frac{\sqrt{(b-c)^2 + 4d^2} + c + a}{a + b}, \tag{4}$$

$$f = \frac{a}{a + b}. \tag{5}$$

The dimensions of a, b, c, and d describing the microgroove are illustrated in Figs. 3(b) and 3(c).

Through moving the 3D micro-stage, the positions of microstructures on fabricated PDMS surface were marked in micro-scales using the optical microscope with different objectives, obtaining the dimensions (i.e., a, b, c, and d) of fabricated PDMS surfaces (data are not shown). Therefore, using Eqs. (4) and (5), the values of r and f are calculated. The CA of the water droplet, in two different models, on these rough PDMS surfaces can be calculated using Eqs. (1) and (3). In Fig. 3(a), the black squares and red squares show the CA for water obtained from the Cassie model and Wenzel model, respectively. Figure 3(a) shows that the CAs of water droplets on the rough PDMS surface have a similar tendency (i.e., CA decreasing with the increasing pitches between two adjacent lines) but have big errors between the experimental results and theoretical results for the range 0–150 μm. For the 150–400 μm range, the experimental results [i.e., blue triangles in Fig. 3(a)] are in good agreement with the results from Wenzel model and Cassie model, especially the latter. Therefore the Cassie model is more suitable to explain the superhydrophobicity of pulsed-laser irradiated PDMS surfaces in our work. The errors between the experimental results of our work and the results from the Cassie model are due to the absence of LIPSS considerations in the calculations because the dimensions of the pulsed-laser irradiated surfaces are only measured on the microscale using the optical microscope.

Raman spectra were also obtained to investigate the effect of the change in chemical composition on the wettability of pulsed-laser irradiated surfaces. Figure 4 shows the Raman spectra obtained under different laser powers. The scanning speed and pitch between two

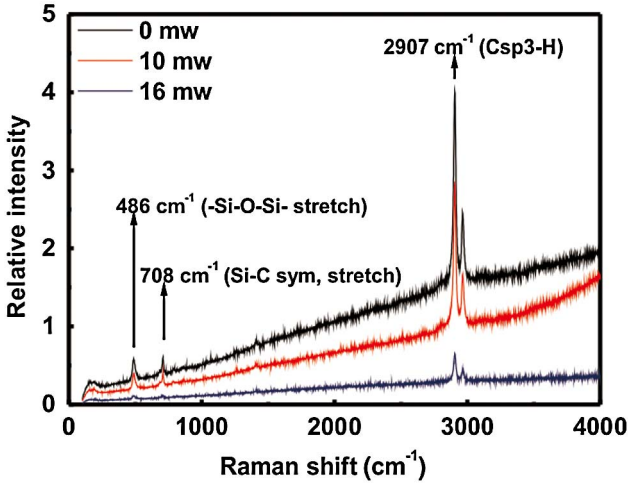

Fig. 4. Raman shift of the PDMS at different laser powers.

adjacent microgrooves were again fixed at 1 mm/s and 15 μm, respectively, for this case. Maximum absorption is observed at 2907 cm^{-1}, which corresponds to the stretching vibration absorption peak of Csp3–H. In comparison to the spectra of nonirradiated PDMS, the intensity of Csp3–H is reduced as the laser power increases. The absorption bands[21] at 486 cm^{-1} (Si–O–Si stretch) and at 708 cm^{-1} (Si–C symmetrical, stretch) weaken as the laser power increases. Hydrophobic functional groups, such as Csp3–H, Si–O–Si, and Si–C, are slightly reduced because of laser ablation, but no new Raman peak is observed in the spectra. Thus, from Fig. 4 it can be basically shown that the superhydrophobic property could be largely attributed to the enhancement of surface roughness because the chemical changes have limited effects on the enhancement of the hydrophobic property.

Besides investigating the effect of PDMS surface morphology on the wettability, the anisotropic wetting behavior of the water droplet on the pulsed-laser irradiated PDMS surface was also studied, where the CA was measured from two different directions. Figure 5(a) shows the water CA as a function of laser power in two orthogonal directions. The scanning speed and pitch between two adjacent microgrooves were fixed at 1 mm/s and 110 μm, respectively. The red squares in Fig. 5 are CAs measured by viewing the water droplet along the direction of the microgroove (i.e., CA $\theta_{\parallel}$), and the black squares represent CA from a direction perpendicular to the microgroove (i.e., CA $\theta_{\perp}$). As the laser power increases from 3 to 150 mW, CA $\theta_{\parallel}$ measured along the direction of microgroove increases from 136° to 153°, and CA $\theta_{\perp}$ measured from the direction perpendicular to the microgroove increases from 136° to 149°. Figures 5(b) and 5(c) show the side view images of the same water droplet on the pulsed-laser irradiated surface captured from two orthogonal directions. CA $\theta_{\parallel}$ [Fig. 5(c)] is larger than CA $\theta_{\perp}$ [Fig. 5(b)] by 4°. This difference in the CAs measured from two orthogonal directions for the same water droplet on the surface is induced by the anisotropic surface roughness. The anisotropic wetting behavior has been previously reported[22] and can be explained by the squeezing effect of the surface roughness, in which the three-phase contact line of the water droplet on the surface is pinned on the surface edge, and the energy barriers increase between the irradiated surface and the nonirradiated surface. This increase in energy barriers prevents the water droplet from spreading along the perpendicular direction of the microgroove. The water droplet can spread more easily along the direction of the microgroove than in the direction perpendicular to the microgroove because of this effect. Therefore, the anisotropic roughness on the irradiated surface can induce the anisotropic wetting behavior of the PDMS surface, which cannot be observed on the nonirradiated surface of the PDMS.

Figures 3 and 5 demonstrate that the hydrophobic property of pulsed-laser irradiated PDMS surfaces can be enhanced by tuning the pitch between two adjacent microgrooves and the laser power. However, to our knowledge, further investigation of the temporal evolution of the wetting behavior of water droplet on the PDMS sample has not been conducted thus far. In this work, we have found that the enhancement of the hydrophobic property does not occur immediately when the sample is irradiated by a pulsed laser in the time-evolution experiments. Figures 6 and 7 show the temporal evolution of the side views of the water droplet on the pulsed-laser irradiated surface, which is captured from directions perpendicular

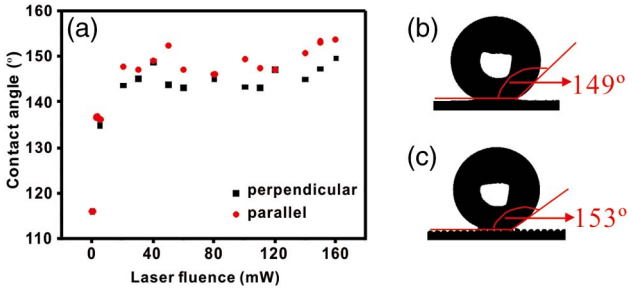

Fig. 5. (a) CA of the PDMS surface as a function of the laser power measured from two orthogonal directions; image of a water droplet on an irradiated surface viewed (b) from the direction perpendicular to the microgroove and (c) from the direction parallel to the microgroove.

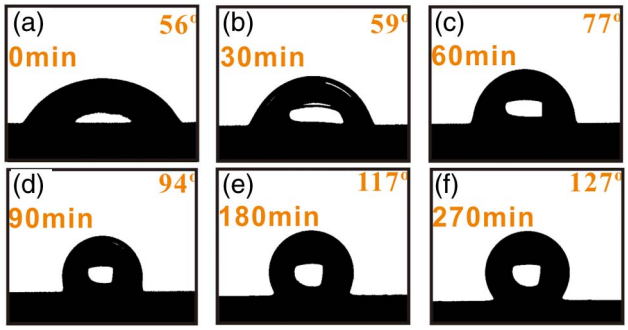

Fig. 6. Evolution of the CA of the surface (after irradiated by femtosecond laser) measured from the direction perpendicular to the microgrooves.

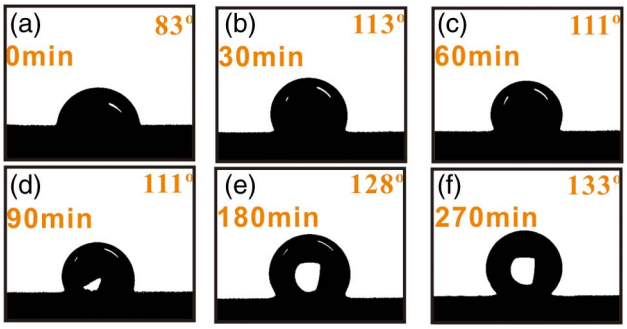

Fig. 7. Evolution of the CA of the surface (after irradiated by femtosecond laser) measured from the direction parallel to the microgrooves.

and parallel to the microgrooves. The laser power, scanning speed, and pitch between two adjacent microgrooves were set at 10 mW, 1 mm/s, and 110 μm, respectively. It is shown that the wettability of the pulsed-laser irradiated surface changes from hydrophilicity to superhydrophobicity. Figure 8 also depicts that the pulsed-laser irradiated surface is anisotropic hydrophilic, with CA $\theta_{\perp}$ of 55° and CA $\theta_{\parallel}$ of 86° in the first minute after laser irradiation. Approximately 6 h after laser direct writing, the irradiated surface exhibits an improvement in the hydrophobic property with CA $\theta_{\parallel}$ of 126° and CA $\theta_{\perp}$ of 130°. For the anisotropic wetting behavior of a water droplet on the pulsed-laser irradiated surface, CA $\theta_{\parallel}$ is always larger than CA $\theta_{\perp}$ at any given time. This temporal evolution of wettability shows that the laser-irradiated PDMS surface is not stable at its first few hours after pulsed laser irradiation.

In conclusion, pulsed-laser irradiation is a highly promising method for fabricating 2D or 3D structures on different materials. In this work, we use this method to produce 2D micro/nanostructures on PDMS surfaces. By varying the laser power and pitch between two adjacent microgrooves, anisotropic dewetting PDMS surfaces with different CAs ranging from 116° to 156° are manufactured. Raman spectra analysis verifies that the superhydrophobicity of the pulsed-laser irradiated surface is mainly due to the enhanced surface roughness rather than the changes of chemical composition. These

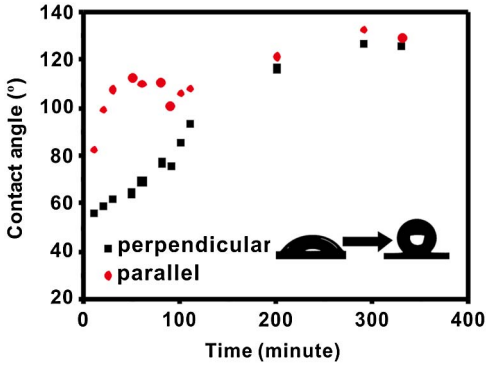

Fig. 8. Evolution of the CA of the irradiated surface measured from directions perpendicular and parallel to the microgrooves.

pulsed-laser irradiated surfaces exhibit anisotropic superhydrophobicity, where CA $\theta_{\parallel}$ is always larger than CA $\theta_{\perp}$. The temporal evolution of the wettability on the pulsed-laser irradiated PDMS surface can help us better understand the changes in the surface chemical composition within 6 h after laser irradiation, which can pave the way to investigate interactions between the polymer and pulsed-laser irradiation. These anisotropic superhydrophobic PDMS surfaces fabricated through pulsed-laser irradiation may also be useful in self-cleaning, liquid transportation without loss, as well as in micro-fluidic channels.

This work was supported by the National Natural Science Foundation of China (Nos. 61178024 and 11374316) and the National Basic Research Program of China (No. 2011CB808103). Q. Zhao acknowledges research funding from the Shanghai Pujiang Program (No. 10PJ1410600).

References

1. Y. T. Cheng, D. E. Rodak, C. A. Wong, and C. A. Hayden, Nanotechnology **17**, 1359 (2006).
2. R. A. Potyrailo, H. Ghiradella, A. Vertiatchikh, K. Dovidenko, J. R. Cournoyer, and E. Olson, Nat. Photonics **1**, 123 (2007).
3. C. H. Sun, P. Jiang, and B. Jiang, Appl. Phys. Lett. **92**, 061112 (2008).
4. D. Wu, J. N. Wang, S.-Z. Wu, Q.-D. Chen, S. Zhao, H. Zhang, H.-B. Sun, and L. Jiang, Adv. Funct. Mater. **21**, 2927 (2011).
5. C. Li, R. Guo, X. Jiang, S. Hu, L. Li, X. Cao, H. Yang, Y. Song, Y. Ma, and L. Jiang, Adv. Mater. **21**, 4254 (2009).
6. G. Piret, E. Galopin, Y. Coffinier, R. Boukherroub, D. Legrand, and C. Slomianny, Soft Matter **7**, 8642 (2011).
7. Y. Sheng, W. Wang, and P. Chen, J. Phys. Chem. C **114**, 454 (2009).
8. R. N. Wenzel, Ind. Eng. Chem. **28**, 988 (1936).
9. A. B. D. Cassie and S. Baxter, Trans. Faraday Soc. **40**, 546 (1944).
10. S. H. Kim, J. H. Kim, B.-K. Kang, and H. S. Uhm, Langmuir **21**, 12213 (2005).
11. R. Asmatulu, M. Ceylan, and N. Nuraje, Langmuir **27**, 504 (2010).
12. Y. Lee, S. H. Park, K. B. Kim, and J. K. Lee, Adv. Mater. **19**, 2330 (2007).
13. X. Guo, Q. Zhao, R. Li, H. Pan, X. Guo, A. Yin, and W. Dai, Opt. Express **18**, 18401 (2010).
14. X. C. Wang, Y. L. W. Linda, Q. Shao, and H. Y. Zheng, J. Micromech. Microeng. **19**, 085025 (2009).
15. Y. Shen, D. Liu, W. Zhang, G. F. Dearden, and K. Watkins, Chin. Opt. Lett. **11**, 021403 (2013).
16. S. Zhang, X. Hu, Y. Liao, F. He, C. Liu, and Y. Cheng, Chin. Opt. Lett. **11**, 033101 (2013).
17. Y. Ju, C. Liu, Y. Liao, Y. Liu, L. Zhang, Y. Shen, D. Chen, and Y. Cheng, Chin. Opt. Lett. **11**, 072201 (2013).
18. T. O. Yoon, H. J. Shin, S. C. Jeoung, and Y.-I. Park, Opt. Express **16**, 12715 (2008).
19. L. Romoli, C. A. A. Rashed, G. Lovicu, G. Dini, F. Tantussi, F. Fuso, and M. Fiaschi, CIRP Ann. Manuf. Technol. **63**, 229 (2014).
20. E. Rebollar, J. R. Vazquez de Aldana, I. Martin-Fabiani, M. Hernandez, D. R. Rueda, T. A. Ezquerra, C. Domingo, P. Moreno, and M. Castillejo, Phys. Chem. Chem. Phys. **15**, 11287 (2013).
21. M. T. Khorasani, H. Mirzadeh, and P. G. Sammes, Radiat. Phys. Chem. **47**, 881 (1996).
22. Y. Zhao, Q. Lu, M. Li, and X. Li, Langmuir **23**, 6212 (2007).